Published in : Macromolécules (2025)
DOI: 10.1021/acs.macromol.5c00718
Status : Postprint (Author's version)

SOLVENT-FREE SYNTHESIS OF ROOM-TEMPERATURE CURABLE NONISOCYANATE POLYURETHANE ADHESIVES AND COATINGS

Luca Narducci[1], Thomas Habets[2], Quentin Grossman[3], Bruno Grignard[4], Michael A. R. Meier[5], and Christophe Detrembleur[6]

1. *Center for Education and Research on Macromolecules (CERM), CESAM Research Unit, University of Liège, Liège 4000, Belgium; Institute of Organic Chemistry (IOC) and Institute of Biological and Chemical Systems-Functional Molecular Systems (IBCS-FMS), Karlsruhe Institute of Technology, Karlsruhe 76131, Germany*
2. *Center for Education and Research on Macromolecules (CERM), CESAM Research Unit, University of Liège, Liège 4000, Belgium*
3. *Mechanics of Biological and Bioinspired Materials Laboratory, Department of Aerospace and Mechanical Engineering, University of Liege, Liege 4000, Belgium*
4. *Center for Education and Research on Macromolecules (CERM), CESAM Research Unit, University of Liège, Liège 4000, Belgium; FRITCO2T Platform, University of Liège, Liège 4000, Belgium ; orcid.org/0000-0002-6016-3317*
5. *Institute of Organic Chemistry (IOC) and Institute of Biological and Chemical Systems-Functional Molecular Systems (IBCS-FMS), Karlsruhe Institute of Technology, Karlsruhe 76131, Germany ; orcid.org/0000-0002-4448-5279*
6. *Center for Education and Research on Macromolecules (CERM), CESAM Research Unit, University of Liège, Liège 4000, Belgium; WEL Research Institute, Wavre 1300, Belgium ; orcid.org/0000-0001-7849-6796*

ABSTRACT

Because of the high risks to human health that arise from the use of isocyanates, new regulations concerning the use of these chemicals were implemented in recent years to improve health and safety standards in the workplace. Correspondingly, the attention of polymer chemists is rapidly shifting from conventional polyurethanes (PUs) to more sustainable and safer nonisocyanate polyurethanes (NIPUs). For applications such as adhesives and coatings, solvent-free NIPU formulations are attractive due to their reduced environmental impact and their potential for use in consumer good applications, but curing typically requires an external heat source due to the low reactivity of the typically applied cyclic carbonate precursors. In this work, solvent-free and ambient-temperature-curing NIPU adhesives and coatings are reported. Two-component (2K) NIPU formulations were designed, exploiting the increased reactivity of a liquid CO_2-sourced bis(α-alkylidene cyclic carbonate) monomer, which was polymerized with a low-viscosity polyamine cross-linker under solvent-free conditions. The composition was varied, adding coreagents to the mixture to diversify the chemical structure of polymer networks. The properties of the thermosets were evaluated at different curing time, revealing high adhesion on aluminum joints already after 1 day of room-temperature hardening. The bonding performance was also tested on different substrates, further evaluated after the incorporation of catechol groups into the polymer matrix, and benchmarked against commercial solvent-free PU glues.

Published in : Macromolécules (2025)
DOI: 10.1021/acs.macromol.5c00718
Status : Postprint (Author's version)

The easy handling, prolonged pot life, negligible VOC, and fast curing at low temperature make the new 2K formulations a competitive alternative to isocyanate-based products, paving the way to new room-temperature NIPU-based adhesives and coatings.

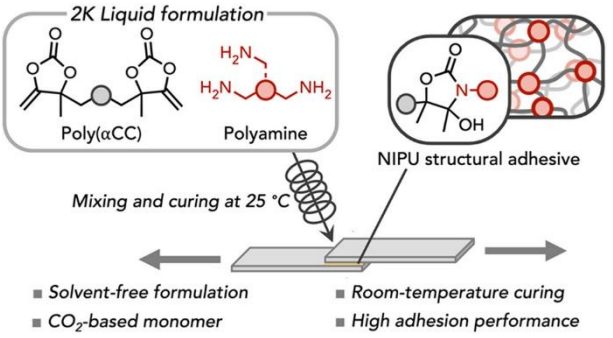

Published in : Macromolécules (2025)
DOI: 10.1021/acs.macromol.5c00718
Status : Postprint (Author's version)

Introduction

Due to their versatile derivatization possibilities and facile cross-linking reactions,[1] polyurethane (PU) resins are among the most common polymers employed for applications such as coatings and adhesives, with a global market size estimated at USD 10.33 billion for PU adhesives [2] and 20.9 billion for PU coatings in 2024. [3] The robustness and versatility of isocyanate chemistry enable tailoring the properties of PUs to suit applications in many different sectors such as automotive, aerospace, electronics, packaging, construction, and textiles. Commonly, PU formulations are composed of polyols, isocyanate hardeners, and a catalyst (Scheme 1A). Despite the widespread use of PUs, their production raised significant concerns related to acute toxicity as well as the phosgenederived nature of isocyanates. To address these issues, new regulations such as REACH impose restrictions and mandate stricter safety precautions for their utilization. [4] Consequently, PU manufacturers must urgently shift away from isocyanate chemistry, and researchers' efforts are currently directed toward the development of nonisocyanate polyurethanes (NIPUs).

The most popular and promising synthetic method for obtaining NIPUs is the polyaddition between poly(cyclic carbonate)s and polyamines to produce poly(hydroxy-urethane)s (PHUs). [5,6] To fabricate PHU adhesives and coatings, several processing methods were reported, such as waterborne, solvent-based, and solvent-free processes. [7] In particular, the latter stands out for a low VOC (volatile organic compound) emission thanks to the absence of organic solvents in the formulation, which dramatically decreases the carbon footprint and potential health risks of the product. On the other hand, the production of solvent-free PHUs is limited by the low reactivity of the typically employed 5-membered cyclic carbonate precursors, much less reactive than isocyanates. A thermal treatment is thus necessary to reach complete curing of the network, while this can be commonly achieved with isocyanate-based formulations at RT. [8-15]

Scheme 1. *Curing of Solvent-free Adhesives at Room Temperature: Comparison of Conventional PUs (A) and NIPU "Mimic" Formulations (B)*

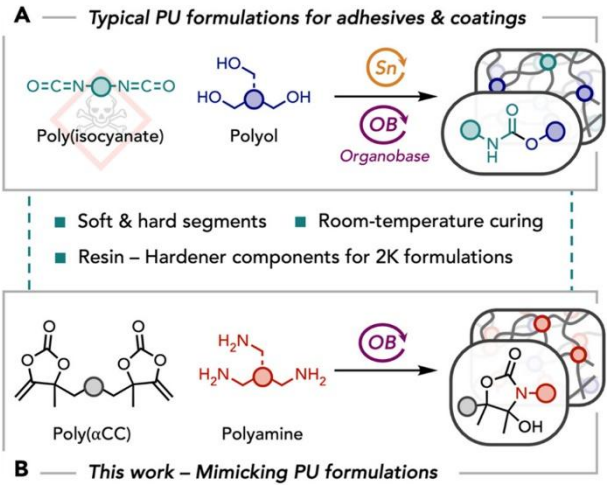

Published in : Macromolécules (2025)
DOI: 10.1021/acs.macromol.5c00718
Status : Postprint (Author's version)

Recently, water has been demonstrated to be not only an effective catalyst for the aminolysis of cyclic carbonates[16] but also an extraordinary solvent for the waterborne curing of PHUs at RT under optimized pH conditions, with short and tunable gel times (2–20 min).[17−19] However, this could only be achieved using water-soluble precursors to deliver highly hydrophilic polymeric coatings with the need to evaporate water as solvent.[17−19] This process was highly efficient for providing hydrophilic coatings, for example, for indoor air purification (formaldehyde capture); however, it was not adapted to design coatings from hydrophobic monomers and formulations.[19]

A practical solution to decrease the curing temperature of solvent-free PHUs was to resort to orthogonal/hybrid chemistries that could overcome the reactivity limits of cyclic carbonates.[7,20,21] Even if this strategy constitutes an attractive alternative to achieve faster curing and tunable properties, developing PHUs that can compete with commercial PUs remains a major challenge,[22] especially for ambient-temperature and solvent-free applications. A promising example of a fast-curing process giving access to PHU thermosets at rather low temperatures was described by Ritter et al. by using the highly reactive triethylenetriamine cross-linker. The curing was performed at 40 °C; however, adhesive strength and coating performance were not evaluated.[23] Attempts to address the low reactivity of PHU formulations were based on the design of more reactive cyclic carbonates with larger rings or bearing electron-withdrawing groups or unsaturations, the specific use of amines of high reactivity, and catalysis.[24−35] Despite these efforts, efficient RT curing has not yet been demonstrated, especially for producing adhesives and coatings.

In contrast, CO_2-based α-alkylidene cyclic carbonates possess an outstanding reactivity toward primary and secondary amines, leading to the formation of either hydroxy-oxazolidones or oxo-urethanes, respectively, new classes of isocyanate-free urethanes.[36] The polymerizations of bifunctional monomers occurred at RT under catalyst-free conditions but required a solvent as the cyclic carbonates were solid compounds in most cases.[37−41] They were exploited to produce linear poly(hydroxy-oxazolidone) or poly(oxo-urethane) polymers but never applied to NIPU thermosets.

In this work, we report the preparation of novel NIPU adhesives and coatings from solvent-free formulations at RT, mimicking PU chemistry through the use of a highly reactive liquid bisαCC monomer (Scheme 1B). After mixing bisαCC with polyamines, the gel time could easily be tuned by a smart choice of the polyamine's chemical structure. Short gel times were obtained for short-chain, reactive polyamines, and longer gel times were reached using longer chain and sterically more hindered polyamines, enabling the application of the formulation onto the surface toward adhesive and coating applications. An organobase catalyst (1,8-diazabicyclo[5.4.0]undec-7-ene; DBU) and low-molecular-weight amine hardeners were introduced to the formulation to further tune the gel time and the thermomechanical properties of the polymers. The adhesive and coating performances of the formulations were finally assessed and benchmarked to those of commercial PU products.

Published in : Macromolécules (2025)
DOI: 10.1021/acs.macromol.5c00718
Status : Postprint (Author's version)

Experimental Section

MATERIALS AND METHODS.

Reagents and Materials. 3-Buten-2one (containing hydroquinone as stabilizer, 90%), 2,2′(ethylenedioxy)diethanethiol (95%), ethynylmagnesium bromide solution (0.5 M in THF), tris(2-aminoethyl)amine (96%), trimethylolpropane tris[poly(propylene glycol), amine terminated] ether (polyetheramine T-403, average Mn 440 g/mol), m-xylylenediamine (99%), 5-amino-1,3,3-trimethylcyclohexanemethylamine (mixture of cis and trans, ≥ 99%), poly(propylene glycol) bis(2aminopropyl ether) (average Mn ∼ 400 g/mol), 1,8diazabicyclo[5.4.0]undec-7-ene (DBU) (≥99%), and copper iodide (≥98%) were purchased from Sigma-Aldrich. Diethylenetriamine (>98%), triethylenetetramine (<90%), 3,3′-diaminodipropylamine (>98%), tetraethylenepentamine (mixture of branched chain isomers and cyclic compounds), and 4,4′-methylenebis(2-methylcyclohexylamine) (mixture of isomers) were purchased from TCI. 2-(3,4Dihydroxyphenyl)ethylamine hydrochloride (dopamine hydrochloride) was purchased from Fluorochem Ltd. Carbon dioxide (CO2) N45 was supplied by Air Liquid.

1 kD Spectra/Por 7 Dialysis Tubing (1 kDa) was purchased from REPLIGEN. Aluminum alloy (5754, or AlMg3) and stainless steel (S235JR) bars were prepared by cutting the material into rectangular pieces (6 × 1.5 × 0.3 cm for aluminum substrates and 6 × 1.5 × 0.1 cm3 for stainless steel ones). Wood substrates (oak, 6 cm × 1.5 cm × 1.7 cm) were purchased from BigMat Cataldo (Belgium); highdensity polyethylene substrates (K46-06-185, 6 cm × 1.5 cm × 0.3 cm) were provided by INEOS (Belgium); poly(methyl methacrylate) substrates (6 cm × 1.5 cm × 0.3 cm) were provided by Superplastic (Belgium). Aluminum alloy (Al 2024-T3) panels were provided by SONACA (Belgium) and prepared by cutting the material into rectangular pieces (6 cm × 5 cm × 0.1 cm).

TEROSON PU 6700 was purchased from Henkel. HUNTSMAN ARALDITE 2028-1 was purchased from Epoxidharze Andreas Weigel (Raschau-Markersbach, Germany).

3-Buten-2-one was purified by distillation prior to use. 4,4′-(6,9Dioxa-3,12-dithiatetradecane-1,14-diyl)bis(4-methyl-5-methylene-1,3dioxolan-2-one) (bisαCC) was synthesized adopting the protocol described by Detrembleur and co-workers.[42]

General Procedure for the Synthesis of Linear NIPUs. Liquid bisαCC (462.6 mg, 1.0 mmol, 1 equiv) was added to a reaction tube together with a solution of diamine (1.0 mmol, 1 equiv) and DBU (30.4 mg, 0.2 mmol, 0.2 equiv). The solvent-free mixture was stirred until vitrification and stored at 25 °C under air. After 24 h, an aliquot of the crude product was withdrawn for ^{1}H NMR and SEC characterizations.

Water-insoluble linear polymers (PA1 and PA2) were solubilized in an acidic solution of formic acid in THF (2 mL, 0.5 M) to quench the polymerization reaction and subsequently precipitated in water and freeze-dried. To guarantee the complete removal of the catalyst and acid, these operations were repeated without using formic acid. Afterward, the samples were solubilized in THF and dialyzed in the

Published in : Macromolécules (2025)
DOI: 10.1021/acs.macromol.5c00718
Status : Postprint (Author's version)

same solvent for 24 h with a 1 kDa porous membrane. The polymers were precipitated in diethyl ether, recovered by filtration, and dried overnight under a vacuum at 55 °C.

Linear polymers that were partially soluble in water (PA3) were solubilized in an acidic solution of formic acid in THF (1 mL, 1 M) to quench the polymerization reaction, subsequently precipitated in water, and freeze-dried. Afterward, the samples were solubilized in THF and dialyzed in the same solvent for 24 h with a 1 kDa porous membrane. The polymers were precipitated in hexane, recovered by filtration, and dried overnight under vacuum at 55 °C.

Linear polymers that were soluble in water (PA4) were solubilized in an acidic solution of formic acid in THF (2 mL, 0.5 M) and dialyzed in water for 24 h with a 1 kDa porous membrane. The solutions were freeze-dried, and the solids were solubilized in THF, precipitated in hexane, and dried overnight under vacuum at 55 °C.

Preparation of NIPU Adhesives, Coatings, Freestanding Films, and Shore Hardness Test Specimens.

Liquid bisαCC was added to a vial together with a mixture of polyamines and DBU at room temperature, and the formulation was then stirred for 50 s. For catechol-containing formulations, a precise amount of dopamine hydrochloride was premixed with DBU and Jeffamine T-403 (dopamine percentage, DOP%, calculated considering the total number of amino groups). Once a homogeneous mixture was obtained, a precise amount of this solution was added to a vial containing bisαCC. Each formulation, with or without dopamine, was prepared keeping an equimolar ratio between cyclic carbonate and amino functional groups, and the catalyst loading was calculated considering the total number of amino and cyclic carbonate reactive groups.

After stirring, the NIPU formulations were processed according to their application: for adhesive samples, the mixture was immediately applied to the substrate for lap-shear testing; for coating samples, the mixture was deposited on an aluminum panel and spread using a casting knife film applicator (ASTM D823) to obtain a coating thickness around 250 μm; for freestanding films, the mixture was poured into a Teflon mold (4 × 2.5 × 0.1 cm3); for Shore hardness test specimens, the mixture was poured in a cylindrical silicone mold (0.8 cm in height, 1.5 cm in diameter).

The polymeric coatings were characterized by cross-cut adhesion test and water contact angle measurements, while the freestanding films were exploited for thermal characterization, tensile testing, and evaluation of the swelling behavior and gel content. Each formulation was tested after 1 day and/or 7 days of curing at 25 °C.

Surface Treatments.

The substrates used for cross-cut and lapshear tests were treated to remove surface impurities that could alter the evaluation of the coating and adhesion performance. Aluminum bars and panels were treated following a procedure previously reported by the authors:38 the substrate was first immersed

Published in : Macromolécules (2025)
DOI: 10.1021/acs.macromol.5c00718
Status : Postprint (Author's version)

into a basic aqueous bath (NaOH 40 g L−1) for 1 min and then into an acidic aqueous bath (73 wt % water, 25 wt % H2SO4, 2 wt %

Na2Cr2O7) for 1 min; at the end of each step, the material was washed with distilled water and wiped with tissue paper. Stainless steel, wood, and polyethylene substrates were cleaned with an acetone/ isopropanol mixture (1:1 v/v) and then with distilled water; poly(methyl methacrylate) substrates were cleaned only with distilled water. The surface of the substrates was wiped with tissue paper after each washing. The procedure was repeated three times, and the substrates were dried at room temperature for 1 h.

Preparation of Lap-Shear Samples.

Single-lap joints were prepared to assess the shear strength of 2K NIPU and commercial PU adhesives. For NIPU adhesives, each formulation was mixed for 50 s and quickly applied on one extremity of the pretreated substrate, depositing around 45 mg of product over a gluing area of 225 mm^2. The second bar of substrate was then immediately put on top of the first one, exerting enough pressure to evenly distribute the adhesive over the overlapped area, without forming defects or squeezing the mixture out of the joint. The specimen was then cured at 25 °C for 1 day or 7 days. For commercial PU adhesives, the preparation procedure was identical, except that reagent mixing was performed using the static mixer supplied with the product.

CHARACTERIZATION TECHNIQUES.

Rheological Measurements. The rheological behavior of the 2K formulations was studied with a rotational rheometer ARES-G2 from TA Instruments, executing time sweep measurements with a parallel plate geometry and at constant strain deformation (1%) and frequency (1 Hz).

Fourier-Transform Infrared Spectroscopy.

Infrared spectra were measured on a Nicolet IS5 spectrometer (Thermo Fisher Scientific) equipped with a diamond attenuated transmission reflectance (ATR) device. For each sample, 32 scans were recorded over the range of 4000−550 cm^{-1} with a resolution of 4 cm^{-1}.

Nuclear Magnetic Resonance Spectroscopy.

^{1}H- and ^{13}C NMR analyses were performed in DMSO-d_6 at 25 °C on a Bruker 400 MHz spectrometer in the Fourier-transform mode. Sixteen scans for 1H spectra and 512 scans for ^{13}C spectra were acquired.

Size Exclusion Chromatography.

Number-average molecular weight (M_n) and weight-average molecular weight (M_w) of linear NIPUs were determined by size exclusion chromatography (SEC) in dimethylformamide (DMF) containing LiBr (0.025 M) at 55 °C (flow rate: 1 mL/min) using linear polystyrene standards for the calibration. The

Published in : Macromolécules (2025)
DOI: 10.1021/acs.macromol.5c00718
Status : Postprint (Author's version)

analyses were carried out with a Waters chromatograph equipped with three columns (Waters Styragel PSS gram 1000 Å (×2), 30 Å), a dual absorbance detector (Waters 2487), and a refractive index detector (Waters 2414).

Thermogravimetric Analysis.

Thermogravimetric analysis (TGA) was performed on a TGA2 instrument from Mettler Toledo. To determine the degradation temperature, evaluated starting from the end of the dehydration step, approximately 5 mg of sample was heated at 10 °C/min from 30 to 600 °C under a nitrogen atmosphere (20 mL/min). To determine the dehydration temperature of linear polymers, identified from the derivative thermogravimetric curve at the beginning of the mass loss signal, around 5 mg of sample was heated at 2 °C/min from 30 to 250 °C under a nitrogen atmosphere (20 mL/min).

Differential Scanning Calorimetry.

Differential scanning calorimetry (DSC) was performed using a DSC 250 differential calorimeter from TA Instruments. Samples of 4 to 6 mg were sealed in hermetic aluminum pans and heated at 10 °C/min from −40 to 120 °C. Subsequently, the samples were cooled to −40 °C at a rate of 10 °C/ min and then reheated at 10 °C/min from −40 to 120 °C (polymers with glass transition temperature close to −40 °C were cooled to −80 °C). All of the experiments were performed under ultrapure nitrogen flow. The glass transition temperature (Tg) was determined using the second heating ramp for linear NIPUs, while the first heating cycle was used for cross-linked NIPUs to prevent modifications of the cross-linking degree at high temperature.

Swelling Behavior and Gel Content.

NIPU freestanding films were cut into rectangular pieces (1 × 0.5 cm) and submerged in 20 mL of solvent (distilled water or THF) for 120 h at room temperature. The samples were then removed from the solvent, gently pressed with a piece of paper, weighed, dried at 70 °C for 24 h, and weighed again. Equilibrium water content (EWC) and gel content (GC) were obtained from eqs 1 and 2:

$$EWC(\%) = \frac{(W_s - W_i)}{W_i} \times 100 \quad (1)$$

$$GC(\%) = \frac{W_F}{W_i} \times 100 \quad (2)$$

where W_i is the initial weight, W_s is the weight of the swollen sample, and W_f is the final weight of the dried sample. The measurements were repeated three times for each formulation.

Cross-Cut Adhesion Tests.

The resistance of NIPU coatings to separation from aluminum substrates was evaluated with an ASTM D3359 cross-cut adhesion test (method B). The coatings were cut with an NK2000 tester from NEURTEK, penetrating all the way to the substrate. Specific round blades were used for coating thicknesses

Published in : Macromolécules (2025)
DOI: 10.1021/acs.macromol.5c00718
Status : Postprint (Author's version)

between 121 and 250 μm to make six evenly spaced incisions (3 mm spacing), horizontally and vertically, creating a lattice pattern on the surface (1.8 × 1.8 cm^2). A pressure-sensitive adhesive tape ISO 2409 was applied on the cross-hatch cut and pressed over the area of the incisions. The tape was rapidly removed by vigorously pulling it off at an angle of 180°, and the result was determined by evaluating the percentage of the grid that was affected by the test, from 0% (5B) to more than 65% (0B).

Water Contact Angle Measurements.

The wettability of NIPU coatings was evaluated by contact angle measurements, carried out with water on an OCA-20 apparatus (Dataphysics Instrument GmbH) in the sessile drop configuration. A 15 μL droplet of MilliQ water was deposited on the surface of the coating, and after 1 min, a high-resolution video camera was used to record the angle between the solid surface and the tangent line to the contacting edge of the droplet. For each formulation, the mean contact angle value was obtained from five measurements taken on different spots of the sample surface.

Tensile Testing.

Tensile tests were conducted at 25 °C on an MTS Criterion Model 43 universal test machine equipped with a 1 kN load cell and at a displacement rate of 10 mm/min. For each formulation, Young's modulus (E), ultimate tensile strength (σu), and fracture strain (εf) were estimated by the average values of five rectangularshaped NIPU films (2.5 cm × 0.5 cm × 0.1 cm). A gripping length of 0.8 cm on each side of the sample was maintained constant for the tests. Young's modulus and fracture strain were determined using eqs 3 and 4, respectively,

$$E = \frac{\sigma}{\varepsilon} \tag{3}$$

$$\varepsilon_f = \frac{(L_f - L_i)}{L_i} \times 100 \tag{4}$$

where σ is the tensile stress, ε is the engineering extensional strain, L_f is the length of the sample at fracture, and L_i is the initial length of the sample. E was calculated in the elastic portion of the stress−strain curve until ε = 1%.

Shore Hardness Testing.

Shore A and Shore D hardness tests were realized on the plane surface of cylindrical samples (0.8 cm in height and 1.5 cm in diameter), using two Hildebrand HD3000 durometers, model types A and D, respectively. The hardness values were recorded 10 s after applying the durometer to the material to ensure a stable reading, and the average results were calculated after five determinations at different positions on the specimen.

Published in : Macromolécules (2025)
DOI: 10.1021/acs.macromol.5c00718
Status : Postprint (Author's version)

LIÈGE université

LAP-SHEAR TESTING.

Lap-shear adhesion tests were performed at 25 °C using an MTS Criterion Model 43 universal test machine, equipped with a 30 or 1 kN load cell and at a displacement rate of 2 mm/min. The measurements were repeated five times for each formulation, and the lap-shear strength was calculated using eq 5:

$$\tau = \frac{F}{A} \tag{5}$$

where τ is the lap-shear strength, *F* is the applied force, and *A* is the overlapped area.

Results and Discussion

DEVELOPMENT OF NIPU FORMULATIONS: INVESTIGATION OF THEIR CURING AND CHEMICAL STRUCTURE.

Recently, some of us reported the synthesis of a CO_2-sourced liquid bis*α*CC that was exploited for constructing polythiocarbonate networks at RT under solvent-free conditions.[42] The monomer was synthesized with an overall isolated yield of 85%, following an upscalable process that provided nearly 60 g of reagent in one batch. Herein, we evaluate its copolymerization with various liquid polyamines to produce NIPU coatings and adhesives from a solvent-free formulation (Scheme 2A). It is important to note that the type of linkage formed by aminolysis of bis*α*CC depends on the type of amine used: secondary amines lead to *oxo*-urethane moieties via ringopening, whereas primary amines yield hydroxy-oxazolidones through a subsequent spontaneous cyclization, the rate of which mainly depends on the steric hindrance of the amine (Scheme 2B).[41] The commercially available polyamine crosslinkers tested, that is, 3,3′-diaminodipropylamine (BAPA), tris(2-aminoethyl)amine (TREN), triethylenetetramine (TETA), tetraethylenepentamine (TEPA), and diethylenetriamine (DETA), were very reactive toward bis*α*CC, leading to vitrification within seconds and without any catalyst, a too short time frame not suitable for the preparation and application of homogeneous formulations to a substrate (i.e., for adhesive and coating applications). The polyetheramine T403 (Jeffamine T-403), characterized by a long poly(propylene glycol) (PPG) backbone and sterically more hindered primary amines presented a more moderate reactivity, and the formulation could easily be manipulated and applied onto substrates. The curing was slow at RT, that is, the gel point was not reached after 10 h of reaction (Scheme 2C).

Published in : Macromolécules (2025)
DOI: 10.1021/acs.macromol.5c00718
Status : Postprint (Author's version)

Scheme 2. *Reaction Scheme (A), Mechanistic Details (B), and Substrate Scope (C) for the Screening of Polyamine Cross-Linkers to be Used in Solvent-free NIPU Formulations, with Representation of Possible Linkages Formed and Formulation Reactivity*

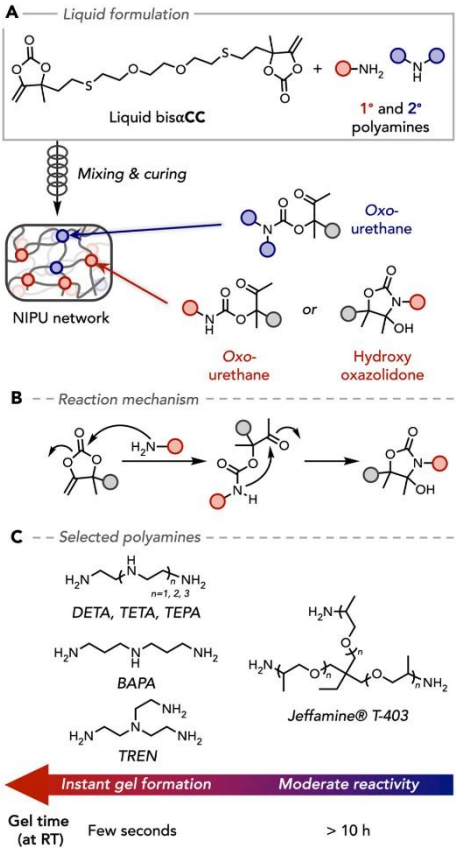

The conditions were therefore explored to shorten the gel time, notably by adding DBUan organobase reported to efficiently catalyze the bis*α*CC aminolysis.[40,41] Although curing at RT was targeted, we have also modulated the temperature to get some insight into its effect on the curing time. An equimolar ratio between amino and cyclic carbonate groups was used for all further formulations, and the evolution of storage (*G*′) and loss (*G*″) moduli was followed over time in all reported conditions (Figure S1). Gel times, defined as the time required to reach the crossover point between *G*′ and *G*″, are reported in Figure 1. Under catalyst-free conditions, the gel times decreased from >10 h at RT to 96 min at 50 °C and 27 min at 75 °C. To accelerate the curing at RT, DBU was added to the formulation. With a DBU content of 5 mol % (vs the total number of amino and cyclic carbonate groups), the gel point was reached within 4.5 h at RT, 12 min at 50 °C and 3 min at 75 °C. The gel time could also be easily tuned by the content of DBU.

Published in : Macromolécules (2025)
DOI: 10.1021/acs.macromol.5c00718
Status : Postprint (Author's version)

Figure 1.

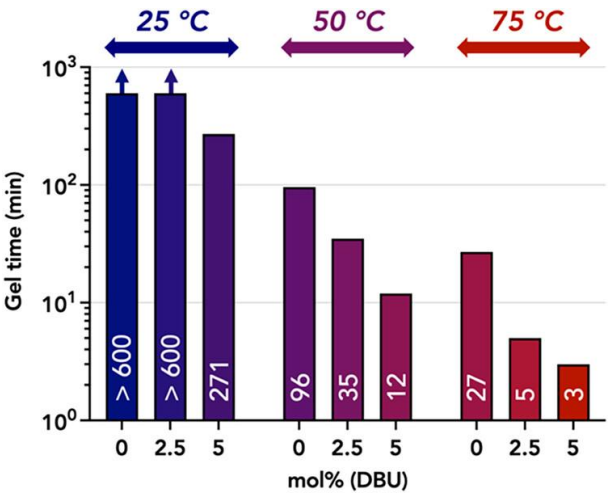

Gel times obtained at different temperatures and catalyst loadings for the bulk polymerization of bisαCC with Jeffamine T-403, calculated without considering 3 min to mix and load the sample into the rheometer.

The curing of the formulation at RT using 5 mol % of DBU as catalyst was monitored using infrared spectroscopy (Figure 2, full spectra shown in Figure S2). The characteristic carbonyl band of the cyclic carbonate at 1822 cm^{-1} and the CC stretching band of the exocyclic olefinic group at 1685 cm^{-1} both decreased as the reaction progressed and disappeared below detection threshold after 72 h. Concurrently, the urethane carbonyl bands (1740 and 1716 cm^{-1}) became increasingly prominent, together with a broad O–H band at around 3400 cm^{-1}, suggesting the formation of hydroxyoxazolidone.

Figure 2.

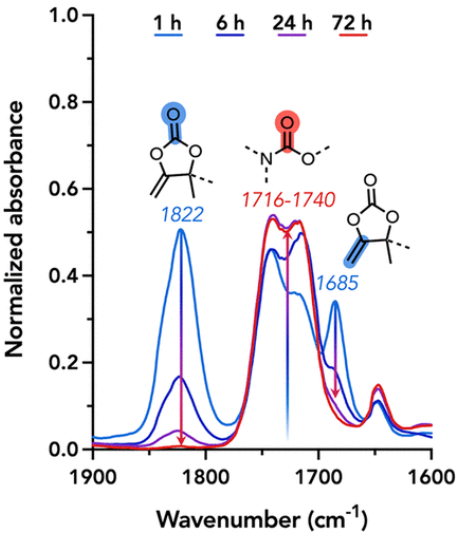

Evolution of characteristic infrared bands in the carbonyl stretching region.

Published in : Macromolécules (2025)
DOI: 10.1021/acs.macromol.5c00718
Status : Postprint (Author's version)

The thermomechanical properties of conventional PU formulations are typically varied by altering the chemical structure of the selected monomers, especially the polyols used. In analogy, to mimic PU formulations containing both rigid and soft segments, we incorporated different diamines with varying lengths and rigidities in our formulations: benzylic (*m*-xylylenediamine, A1), cycloaliphatic (isophorone diamine A2; 4,4′-methylenebis(2-methylcyclohexylamine) A3), and polyether (PPG average $M_n \sim 400$ g/mol, bifunctional equivalent of T-403, A4) diamines. In order to identify the nature of the linkages formed during curing the networks (*oxo*urethane vs hydroxy-oxazolidone)that are expected to influence the network propertieslinear polymers were thus synthesized from the different diamines under the same conditions as the polymer networks (RT, neat, 5 mol % DBU, Scheme 3). The crude reaction mixtures were characterized by SEC. The purified linear polymers were characterized by NMR and IR spectroscopy as a point of comparison with the polymer networks, which cannot be dissolved in organic solvents for NMR characterization. The thermal properties of the polymers were assessed by thermogravimetric analysis (TGA) and differential scanning calorimetry (DSC) experiments. The polymer composition, molecular weight, and thermal properties are reported in Table 1.

Scheme 3.

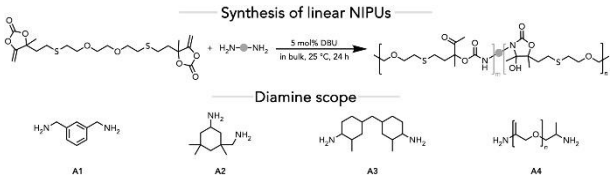

Reaction Scheme and Substrate Scope for the Synthesis of Linear NIPUs from bisαCC

Table 1.

entry	diamine	polymer	hydroxy-oxazolidone/oxo-urethane	M_n(g/mol)[b]	M_w(g/mol)[b]	D[b]	$T_{deg10\%}$ (°C)[c]	T_{dehyd} (°C)[d]	T_g (°C)[e]
1	A1	PA1	100:0	2600	6700	2.7	318	130	36
2	A2	PA2	89:11	1800	4100	2.3	307	142	59
3	A3	PA3	57:43	1700	4000	2.3	279	103	28
4	A4	PA4	100:0	6100	16,700	2.7	297	144	-25

[a] Conditions: bis α CC (1.0 mmol), diamine (1.0 mmol), bulk, 25 °C, 5 mol % DBU vs total NH_2 and CC groups, 24 h. [b] Determined on crude products by SEC in DMF/LiBr. [c]Determined by TGA at 10% mass loss after dehydration, heating the sample at 10 °C/min. [d]Determined by TGA, heating the sample at 2 °C/min. [e]Determined by DSC using the second heating cycle, from -40 to 120 °C at 10 °C/min (for PA4, the cycle started at -80 °C).

Figure 3 shows the overlaid ^{1}H NMR spectra of the purified polymers in DMSO-d_6, focusing on the chemical shift region of the hydroxy-oxazolidone OH signal (at 5.5−6.3 ppm) and the linear urethane NH signal (at 7.1−7.5 ppm) (full ^{1}H NMR peaks assignments and ^{13}C NMR spectra are provided in Figures S3−S10). With A1 and A4, the polymers presented the corresponding poly(hydroxy-oxazolidone) structures with all typical resonances. As A4 can be considered a bifunctional equivalent of Jeffamine

Published in : Macromolécules (2025)
DOI: 10.1021/acs.macromol.5c00718
Status : Postprint (Author's version)

T-403 with similar reactivity, it is suggested that polymer networks PJ are similarly mainly composed of hydroxy-oxazolidone linkages. The copolymerization of sterically hindered A3 resulted in a 43% content of oxourethane (Table 1, entry 3), in agreement with previous studies, demonstrating the presence of both linkages in polymers based on cycloaliphatic diamines.[41] The less hindered A2 only contained 11% of an oxo-urethane linkage, certainly due to the presence of a more accessible amine group (Table 1, entry 2).

Figure 3.

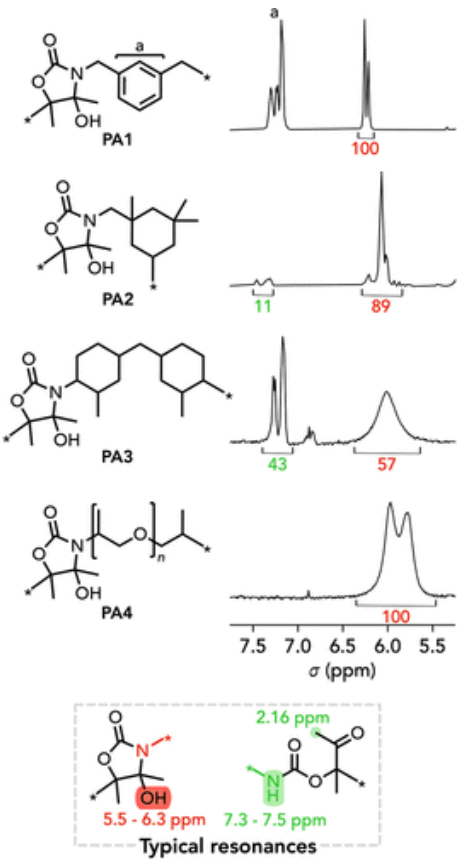

Stacked ^{1}H NMR spectra showing characteristic signals of hydroxy-oxazolidone and oxo-urethane linkages in pure linear NIPUs.

The overlay of the IR spectra of the linear polymers (reported in Figure S11) showed that the position of the C O stretching band depended on the diamine used. Moreover, the same double band as observed in PJ (Figure 2) also appeared in the spectra of PA4, despite the exclusive presence of hydroxy-oxazolidone linkages in the polymer.

SEC characterization of the crude linear polymers showed a range of weight-average molar masses (M_w) from 4.0 to 16.70 kg mol^{-1} (Table 1 and Figure S12). Although the molar mass of the different polymers could not be compared due to different chemical structures and thus hydrodynamic volumes, PA2 and PA3, obtained from the most hindered diamines, displayed comparable molar mass

Published in : Macromolécules (2025)
DOI: 10.1021/acs.macromol.5c00718
Status : Postprint (Author's version)

values. PA4 presented the highest M_w, and PA1 presented an intermediate one. The dispersity ($Đ$) values were overall consistent with the stepgrowth polymerization process.[41] It must be noted that the polymerization media rapidly vitrified, reducing chain diffusion and therefore restricting the polymer molar mass.

In agreement with our previous data,[43,44] the thermogravimetric analysis of purified NIPUs (Figures S13–S16) showed the characteristic dehydration step of the hydroxy-oxazolidone moieties, starting between 100 and 145 °C (Table 1). The thermal degradation temperature at 10% mass loss ($T_{deg10\%}$) ranged between 279 (entry 3) and 318 °C (entry 1). The DSC curves of the polymers (Figures S17) displayed a broad array of glass transition temperatures, from −25 °C with the most flexible diamine A4 to 59 °C with the most rigid isophorone diamine A2 (Table 1, entries 4 and 2). Polymers PA1 and PA3 exhibited intermediate T_gs of 36 and 28 °C, respectively (Table 1).

PREPARATION AND CHARACTERIZATION OF NIPU ADHESIVES AND COATINGS.

The structure of the primary diamines affected the NIPU structure and the linkage selectivity, which could be modulated from exclusive oxazolidone to a mixture of oxazolidone and *oxo*-urethane of different contents. We thus investigated the addition of these diamines to the bisαCC/ Jeffamine T-403 formulation to modulate the properties of the NIPU thermoset. A4 was not added as a comonomer, as we targeted the introduction of more reactive and more rigid amines to the formulation. For each tested diamine, two formulations were prepared by varying the diamine/T-403 molar ratio from 1/4 to 1/3, while keeping the molar ratio of primary amine (NH_2) to cyclic carbonate (CC) groups constant, along with the catalyst loading relative to the total

NH_2 and αCC groups.

RHEOLOGICAL BEHAVIOR AND IR CHARACTERIZATION.

To evaluate the effect of incorporating diamines on the curing rate, the evolution of the formulations' rheological behavior was investigated by monitoring changes in G' and G'' over time. The results of the study are reported in Table 2 and Figure S18.

Published in : Macromolécules (2025)
DOI: 10.1021/acs.macromol.5c00718
Status : Postprint (Author's version)

Table 2. *Gel Time of Cross-Linked NIPUs Obtained by Curing Formulations Composed of bis a CC, Jeffamine T- 403, and a Diamine*[a]

entry	diamine	polymer	diamine/triamine	gel time (min)[b]
1		PJ	0:1	271
2	A1	PJA1a	1:4	214
3		PJA1b	1:3	109
4	A2	PJA2a	1:4	438
5		PJA2b	1:3	217
6	A3	PJA3a	1:4	>600
7		PJA3b	1:3	258

[a]Conditions: NH_2/*a*CC = 1, bulk, 25 °C, 5 mol % DBU vs total NH_2 and *a*CC groups. [b]Calculated without considering 3 min to mix and load the sample since the start of the reaction.

Except for PJA1a (entry 2), formulations with a diamine to triamine ratio of 1:4 displayed a gel time longer than that of PJ, whereas those with a ratio of 1:3 exhibited a shorter gel time. This trend was attributed to the competing effects of the diamines on the gelation rate. On one hand, they reacted faster than Jeffamine T-403 and accelerated the polymerization, and on the other hand, they reduced cross-linking density. Therefore, with PJA2a and PJA3a (entries 4 and 6), the lower cross-linking density compared to PJ resulted in slower gelation, while for PJA1b, PJA2b, and PJA3b (entries 3, 5, and 7), the diamines enhanced the polymerization rate, leading to quicker gelation. Additionally, the gel time followed the reactivity trend of the diamines: A1 exhibited the fastest gelation, followed by A2, and A3 displayed the slowest crosslinking. The IR analysis conducted after 3 days of RT curing revealed no variation in the band position of the carbonyl of urethane across the different formulations (Figure S19).

SWELLING BEHAVIOR, GEL CONTENT, AND COATING PERFORMANCE.

The swelling behavior, gel content, thermal and mechanical properties, and coating and adhesion performance of the cured 2K NIPU formulations were then assessed. To evaluate the performance and properties evolution over time, each analysis was carried out after 1 day and 7 days of curing at RT, and the results are summarized in Tables 3–5.

The equilibrium water content (EWC) and gel content (GC) were determined for NIPU freestanding films, while NIPU coatings were characterized by a water contact anglemeasurement (CA) and cross-cut adhesion test (CCA) (Table3).

Published in : Macromolécules (2025)
DOI: 10.1021/acs.macromol.5c00718
Status : Postprint (Author's version)

Table 3. *Equilibrium Water Content, Gel Content, and Coating Performance of Cross-Linked NIPUs Obtained by Curing Formulations Composed of bisαCC, Jeffamine T- 403, and a Diamine*[a]

				after 1 day					after 7 days				
entry	diamine	polymer	diamine/triamine (n/n)	EWC[b] (%)	GC (%)[c] H_2O	GC (%)[c] THF	CA[d] (°)	CCA[e]	EWC[b] (%)	GC (%)[c] H_2O	GC (%)[c] THF	CA[d] (°)	CCA[e]
1		PJ	0:1	76 ± 1	97.3 ± 0.3	75 ± 1	65 ± 4	4B	86 ± 8	95.2 ± 0.6	79.5 ± 0.2	60 ± 2	5B
2	Al	PJAla	1:4	102 ± 4	96.0 ± 0.6	65.1 ± 0.6	79 ± 4	4B	102 ± 8	92 ± 3	61 ± 1	68 ± 3	5B
3		PJAlb	1:3	111 ± 9	95.2 ± 0.8	62.2 ± 0.8	80 ± 2	4B	116 ± 9	94 ± 1	68 ± 1	74 ± 3	5B
4	A2	PJA2a	1:4	80 ± 1	97.3 ± 0.6	68 ± 2	69 ± 7	3B	100 ± 4	96.6 ± 0.3	73 ± 1	69 ± 2	4B
5		PJA2b	1:3	93 ± 9	96 ± 1	68 ± 2	75 ± 7	3B	112 ± 3	95.3 ± 0.4	70 ± 2	70 ± 3	4B
6	A3	PJA3a	1:4	55 ± 2	98.2 ± 0.2	72 ± 2	78 ± 3	4B	89 ± 3	95.6 ± 0.4	72.1 ± 0.3	68 ± 2	5B
7		PJA3b	1:3	65 ± 3	97.5 ± 0.4	69 ± 1	76 ± 3	3B	97 ± 8	95 ± 1	71 ± 2	69 ± 2	4B

[a] Conditions: NH_2/αCC = 1, bulk, 25 °C, 5 mol % DBU vs total NH_2 and αCC groups. [b] EWC: equilibrium water content of self-standing films submerged in water for 120 h at RT. [c] GC: gel content of self-standing films submerged in water or THF for 120 h at RT and dried at 70 °C for 24 h. [d] CA: water contact angle. [e] CCA: cross-cut adhesion of coatings tested using the ASTM D 3359 test method B.

Published in : Macromolécules (2025)
DOI: 10.1021/acs.macromol.5c00718
Status : Postprint (Author's version)

For the NIPU thermosets obtained after 1 day of curing, the average equilibrium water content (EWC) greatly varied depending on the formulation. The ones derive from A1 exhibited the highest EWC (102 ± 4% for PJA1a, entry 2, and 111 ± 9% for PJA1b, entry 3) and thus the greatest affinity to water, certainly due to their high density of polar hydroxyoxazolidone linkages. The water uptake was lower for PJA2a (80 ± 1%, entry 4) and PJA2b (93 ± 9%, entry 5), while PJ (entry 1), PJA3a (entry 6), and PJA3b (entry 7) were the most resistant to water-swelling (EWC = 76 ± 1, 55 ± 2, and 65 ± 3%, respectively). PJA3a and PJA3b presented the lowest EWC, in line with a higher content of *oxo*-urethane linkages, less hydrophilic than the hydroxy-oxazolidone ones. Increasing the relative amount of diamine and consequently the concentration of urethane groups also increased the water absorption, and thus, EWC increased. These trends were confirmed for samples analyzed after 7 days of curing with EWC values that were generally higher.

Gel contents (GC) in water were high in all cases (92–98%) after 1 and 7 days of curing. They were lower in THF with values between 61 and 79%. The highest value was obtained for the formulation without diamines (PJ, entry 1) after 7 days of curing, which is in line with a higher cross-linking density. The lower GC observed with the other formulations containing the amines mixture suggested the presence of extractable chains or compounds that were solubilized in the solvent. The NMR analysis of the soluble fraction (reported in Figure S20) confirmed the presence of hydroxy ketone functional groups generated by the hydrolysis of the cyclic carbonate by residual water present in the monomers.

NIPU coatings deposited on aluminum substrates presented water contact angles ranging from 65 to 80° (entries 1 and 3) for samples analyzed after 1 day, slightly decreasing to a range between 60° and 74° after 7 days. This slight increase in hydrophilicity with the curing time was in agreement with the increased content of hydroxyl groups from the hydroxyoxazolidone moieties. All formulations exhibited a gradual decrease in the static contact angle over time, while the contact line remained fixed. This behavior is indicative of strong contact line pinning, where the droplet does not recede despite volume loss due to evaporation, suggesting a high level of interaction between the coating surface and water. The adhesion strength of the NIPU coatings was then evaluated by cross-cut tests according to the ASTM D3359 standard. The coating performance improved when the curing time was extended to 7 days, suggesting that the curing was not complete after 1 day. Except for the samples prepared from A2, the cross-cut area was perfectly intact for the coatings tested after 7 days; thus, they were classified as 5B for their high adhesion to the aluminum surface (0% removal of the coating from the substrate). In the case of the polymers obtained from A2, they were characterized by a lower adhesion and were ranked as 4B since some of the squares in the lattice pattern were partially affected by the test, and the superficial layer of the film was removed to some extent while pulling the tape.

The resistance of the coatings to wet delamination was investigated by submerging coated aluminum substrates in distilled water for 48 h. The samples were then placed in an oven at 50 °C for drying, and after 24 h, the cross-cut test was repeated, showing the same coating performance evaluated before the immersion.

Published in : Macromolécules (2025)
DOI: 10.1021/acs.macromol.5c00718
Status : Postprint (Author's version)

THERMAL PROPERTIES.

Table 4 summarizes the degradation temperature ($T_{deg10\%}$) and glass transition temperature (T_g) of the NIPU networks determined by TGA and DSC, respectively.

Table 4. *Thermal Properties of Cross-Linked NIPUs Obtained by Curing Formulations Composed of bis αCC, Jeffamine T- 403, and a Diamine*[a]

				after 1 day		after 7 days	
entry	coreagent	polymer	diamine/triamine (n/n)	$T_{deg10\%}$ (°C)[b]	T_g (°C)[c]	$T_{deg10\%}$ (°C)[b]	T_{g1} (°C)[c]
1		PJ	0:1	268	10	266	10
2	A1	PJA1a	1:4	258	9	239	20
3		PJA1b	1:3	256	11	252	24
4	A2	PJA2a	1:4	266	10	257	22
5		PJA2b	1:3	265	11	256	23
6	A3	PJA3a	1:4	262	8	260	22
7		PJA3b	1:3	262	9	256	19

[a]Conditions: NH_2/αCC = 1, bulk, 25 °C, 5 mol % DBU vs total NH_2 and αCC groups. [b]Determined by TGA at 10% mass loss, heating the sample at 10 °C/min. [c]Determined by DSC using the first heating cycle, from -40 to 120 °C at 10 °C/min

Differently from the corresponding linear polymers, it was not possible to identify a dehydration step in the degradation pattern of NIPU thermosets, and thus, the thermal degradation temperatures at 10% mass loss could not be compared. The products were indeed analyzed without any purification, and the DBU left in the matrix might hamper the loss of water from the polymer network because of an interaction between the basic site of the catalyst and the alcohol moiety of the hydroxyoxazolidone.[38] Cross-linked polymers analyzed after 1 day of curing were characterized by a gradual weight loss starting at around 100 °C, followed by a major degradation step between 300 and 400 °C. Thermosets analyzed after 1 week displayed a different behavior at high temperature since the main degradation was less pronounced, and a certain percentage of the polymer mass (around 15–20% of the initial mass) was retained even above 400 °C, before a final slow decomposition until 600 °C occurred. All the TGA curves are shown in Figures S21–S27, and two representative ones are displayed in Figure 4.

Published in : Macromolécules (2025)
DOI: 10.1021/acs.macromol.5c00718
Status : Postprint (Author's version)

Figure 4.

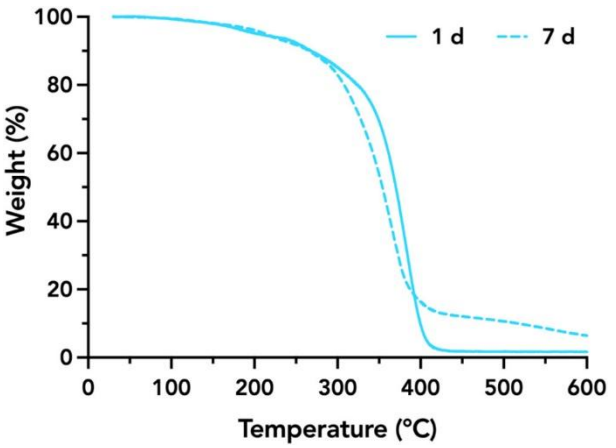

Representative TGA curves of PJ after 1 day (solid curve) and 7 days (dashed curve) of RT curing

Considering the thermal degradation temperatures at 10% mass loss, the difference in composition between formulations did not have a significant impact, that is, the determined $T_{deg10\%}$ values remained within temperatures of 258 °C (PJA1a, entry 2) to 268 °C (PJ, entry 1). Analogous values were measured for fully cross-linked samples, which had a similar degradation pattern until the main mass loss around 300 °C.

Cross-linked NIPUs were analyzed by DSC to determine their glass transition temperature, which was between 8 and 11 °C after 1 day of RT curing using the first heating ramp to prevent modification of the degree of cross-linking (curves reported in Figures S28–S34). The T_g value of thermosets prepared using a coreagent increased after longer curing time, while for PJ (entry 1), it remained constant at 10 °C. This difference was attributed to the reduced macromolecular mobility derived from the presence of low-molecular-weight diamines, less flexible than the long polyether chains of the cross-linker. Interestingly, the influence on the polymer chain mobility was the same for all the diamines, even if the T_g of the respective linear polymers were diverse. However, the glass transition temperature range of the thermosets was compatible with that required for room-temperature adhesives or coatings, that is, ensuring sufficient pliability at the service temperature, where the material should not behave like a brittle solid (far below the T_g) or like a viscous fluid (far above the T_g).

MECHANICAL PROPERTIES.

Table 5 summarizes the mechanical properties of the polymers determined by tensile and hardness tests (stress–strain curves are reported in Section S3.6).

Published in : Macromolécules (2025)
DOI: 10.1021/acs.macromol.5c00718
Status : Postprint (Author's version)

Table 5. *Mechanical Properties of Cross-Linked NIPUs Obtained by Curing Formulations Composed of bisαCC, Jeffamine T-403, and a Diamine*[a]

				after 1 day				after 7 days			
entry	coreagent	polymer	diamine/triamine (n/n)	E (MPa)[b]	σ_u (MPa)[c]	ε_f (%)[d]	shore A hardness	E (MPa)[b]	σ_u (MPa)[c]	ε_f (%)[d]	shore D hardness
1		PJ	0:1	35 ± 10	5.9 ± 1.7	222 ± 32	59	35 ± 6	4.6 ± 1.3	315 ± 17	32
2	A1	PJA1a	1:4	104 ± 40	7.0 ± 1.2	118 ± 44	66	75 ± 20	4.1 ± 0.9	283 ± 10	42
3		PJA1b	1:3	107 ± 39	8.6 ± 1.0	166 ± 49	72	86 ± 30	4.8 ± 1.0	232 ± 78	45
4	A2	PJA2a	1:4	139 ± 32	7.0 ± 1.3	209 ± 39	70	88 ± 13	4.6 ± 0.5	270 ± 23	48
5		PJA2b	1:3	236 ± 49	9.6 ± 1.0	71 ± 24	85	90 ± 5	5.2 ± 0.8	266 ± 32	51
6	A3	PJA3a	1:4	70 ± 29	6.1 ± 0.7	249 ± 25	68	89 ± 14	4.9 ± 0.7	273 ± 16	45
7		PJA3b	1:3	146 ± 56	10.0 ± 1.2	257 ± 61	82	132 ± 25	5.1 ± 0.7	246 ± 9	47

[a]Conditions: NH_2/αCC = 1, bulk, 25 °C, 5 mol % DBU vs total NH_2 and αCC groups. [b]*E*: Young's modulus. [c]u: ultimate tensile strength. [d]f: fracture strain.

The stress–strain curves (shown in Figures S35 and S36) resembled typical flexible plastic polymers: the samples stretched less than 10% of their initial length elastically, before showing a peak stress (yield point), followed by strain softening, extended plastic deformation, hardening, and then fracture. This mechanical behavior was governed by the presence of Jeffamine cross-linker, whose flexibility allowed for an extensive stretching of the network before reaching the fracture point. The use of lower molecular mass diamines as coreagents, however, generated harder and stronger structures characterized by shorter and more compact macromolecular chains and a higher density of polar carbamate linkages.

Among the samples tested after 1 day of curing, PJA2b was the stiffest formulation (E = 236 ± 49 MPa, entry 5) because of the influence of A2, which lent compactness to the network and hindered the elongation when tensile stress was applied. The presence of rigid chains derived from the diamines also translated into a lower elongation at break, especially for PJA2b, which exhibited a brittle behavior, with a low fracture strain (ε_f = 71 ± 24%) and a yield strength coincident with the ultimate tensile strength of the material. Only PJA3a and PJA3b (entries 6 and 7) showed a fracture strain on average higher than that of PJ (entry 1). The effect of the diamine content on the mechanical properties of the thermoset was more pronounced for the mixtures with a 1:3 diamine/triamine ratio, which displayed higher elastic modulus and ultimate tensile strength.

The samples tested after 7 days exhibited similar rigidity, strength, and elongation at break since the influence of the diamines was attenuated for completely cured networks; only PJ had a considerably lower Young's modulus (E = 35 ± 6 MPa) and a higher fracture strain (ε_f = 315 ± 17%). Compared to the samples tested after 1 day, both E and σ_u generally decreased, while the elongation at break greatly increased, resulting in a transition to more ductile, softer materials with an overall lower toughness.

Published in : Macromolécules (2025)
DOI: 10.1021/acs.macromol.5c00718
Status : Postprint (Author's version)

The hardness of the thermosets always increased with the diamine content, the rigid diamine A2 produced the hardest materials, and the softest polymers were obtained with the formulation PJ (entry 1), with hardness values of 59 Shore A after 1 day and 32 Shore D after 7 days of RT curing. Notably, in contrast to the results obtained for the elastic modulus, the hardness increased significantly after 7 days of curing, rising from Shore A to Shore D.

ADHESION PERFORMANCE.

The adhesion of the solvent-free formulations on aluminum substrates was assessed by lap-shear testing (Figure 5A) after 1 and 7 days of RT hardening. Representative force–displacement curves are reported in Figures S37 and S38, and two illustrative examples are shown in Figure 5B. The results of the tests are summarized in Figure 5C,D and Table S1.

Figure 5.

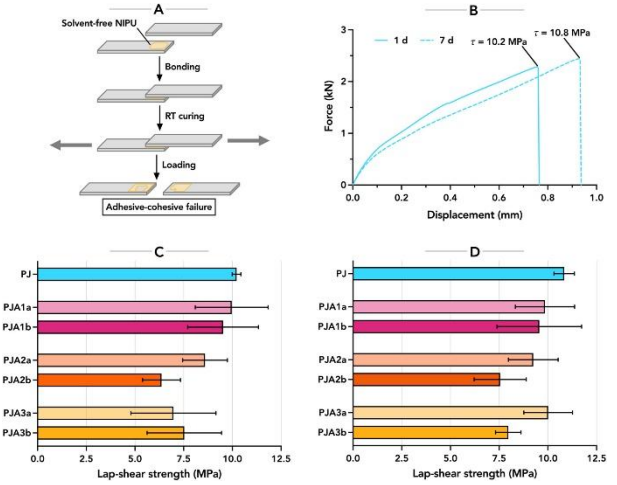

Graphical illustration of the lap-shear test (A); representative force–displacement curves of PJ after 1 day (solid curve) and 7 days (dashed curve) of RT curing (B); lap-shear strength comparison for cross-linked NIPUs, evaluated after 1 day (C) and 7 days (D) of RT curing on aluminum substrates.

Already after 1 day of curing, the 2K adhesives showed excellent adhesion to the substrates, with a lap-shear strength (τ) as high as 10.0 ± 1.3 MPa for PJA1a and 10.2 ± 0.2 MPa for PJ. Polymeric mixtures containing A2 and A3 had lower adhesion strength, especially PJA2b, which was characterized by a shear bonding strength of 6.4 ± 1.0 MPa, confirming the lower adhesive performance noticed with the cross-cut test. Due to the higher cross-linking density, the samples obtained after 7 days displayed better performance on average, with PJ giving the best result (τ = 10.8 ± 0.5 MPa). All the specimens showed a mixed adhesive-cohesive failure (Figure S39), which indicated that cohesive failure and bonding failure between polymer and adherend took place simultaneously. Compared to the mixture that had Jeffamine T-403 as the only polyamine reagent (PJ), the other multicomponent formulations exhibited an inferior performance, and the lap-shear strength was lower when a higher diamine content was used (PJA1b, PJA2b, PJA3b). These results led to the conclusion that a highly cross-linked

Published in : Macromolécules (2025)
DOI: 10.1021/acs.macromol.5c00718
Status : Postprint (Author's version)

and homogeneous network had a crucial role in ensuring strong cohesion of the polymer network and adhesion to the metallic substrate, while the addition of bifunctional polyamines did not positively affect the outcome of the test. PJ outperformed the other formulations, had a pot life of several minutes longer, and gave the most reproducible results, which were comparable after 1 and 7 days of curing; therefore, it was selected as the best-performing formulation to be used for the following experiments.

The gluing properties of PJ, already tested on aluminum alloy (Al), were further evaluated after 1 day of RT curing on other substrates: stainless steel (SS), poly(methyl methacrylate) (PMMA), wood (W), and high-density polyethylene (HDPE). Representative force–displacement curves are reported in Figure S40, and the representative failure modes are shown in Figure S41, while the results of the tests are summarized in Figure 6 and Table S2.

Figure 6.

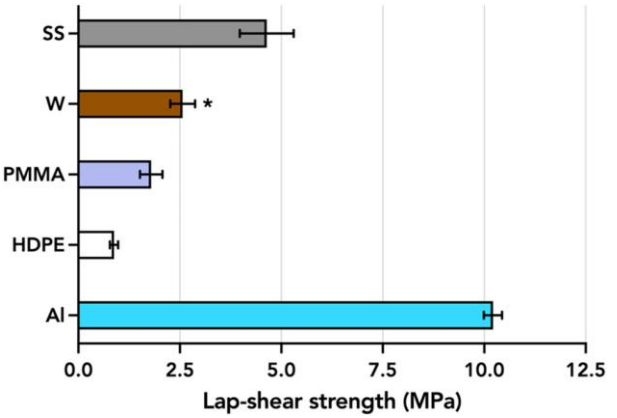

Lap-shear strength of NIPU adhesive formulation PJ, evaluated after 1 day of RT curing on different substrate materials: stainless steel (SS), wood (W), poly(methyl methacrylate) (PMMA), high-density polyethylene (HDPE), and aluminum alloy (Al). *Delamination of wood fibers.

The single-lap-shear tests performed on stainless steel displayed poorer adhesion compared to that on aluminum, with an average lap-shear strength of 4.6 ± 0.7 MPa. A different failure mode was also noticed since some specimens underwent adhesive failure instead of the mixed adhesivecohesive previously observed with Al substrates. The interfacial interaction was also weaker for PMMA and HDPE substrates (τ = 1.8 ± 0.3 and 0.9 ± 0.1 MPa, respectively), which displayed an adhesive failure in all cases. These results were ascribed to the low surface energy of the materials (especially HPDE), which is often reported as one of the main reasons behind the bonding failure of some plastic substrates.[45−48] Lap-shear tests on wood were first performed with 3 mm-thick specimens; however, these substrates broke outside the gluing area (stock-break failure). The thickness of the substrate was consequently increased to 17 mm, and the tests were performed applying tension in parallel to the wood grain direction. After an initial increase of the shear force, delamination of the wood fibers occurred, and the two components of the joint began to slide against each other (as observed in the exemplary force–displacement curve in Figure S40). The failure mode could be described as "light-fiber-tear" failure since a thin layer of wood fibers was removed from the substrate surface by the adhesive, and

Published in : Macromolécules (2025)
DOI: 10.1021/acs.macromol.5c00718
Status : Postprint (Author's version)

the average lap-shear strength was 2.6 ± 0.3 MPa. The real lap-shear adhesion was thus underestimated due to the strong adhesion of the adhesive to wood that delaminated during testing.

As a result of the strong and versatile interactions that the catechol moiety can establish, numerous bioinspired catecholbased adhesives and coatings have been developed over the years.[45,49−51] In particular, mimicking the binding mechanism of marine mussels, a previous study reported a significant improvement in the lap-shear strength of PHU glues containing pendent catechol groups.[10] These mussel-mimetic PHU thermosets were prepared by polyaddition of a trifunctional cyclic carbonate, a liquid diamine, and a catecholamine (dopamine, DOP), which proved to enhance the cohesion of the polymeric structure and the adhesion to the surface of the substrate. Adopting the same strategy for the NIPU formulations described in this work, the adhesion performance was assessed after the addition of various contents of dopamine hydrochloride to the reagent mixture PJ. DBU was expected to deprotonate the ammonium group and release free dopamine, which could then react as a nucleophile with the cyclic carbonate. The NIPU adhesives developed were then benchmarked against two commercial fast-curing solvent-free 2K PU glues, that is, TEROSON PU 6700 and ARALDITE 2028−1, by performing lap-shear tests on aluminum alloy substrates (Al 5754) after 1 day of RT curing (results displayed in Figure 7 and Section S4.1).

Figure 7.

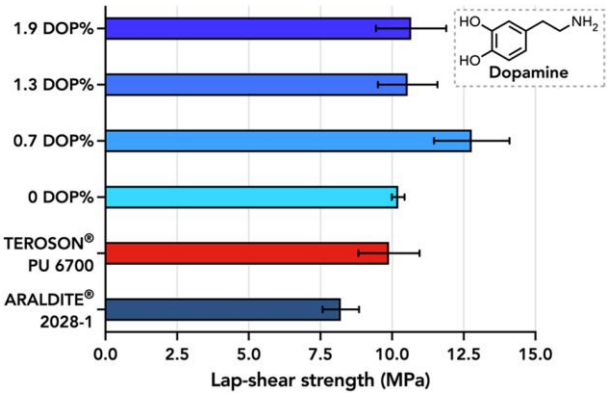

Lap-shear strength comparison for commercial PU adhesives and catechol-containing NIPUs obtained by bulk polymerization of bisαCC with T-403 and dopamine (DOP), evaluated after 1 day of RT curing on aluminum alloy substrates. An equimolar ratio between amino and cyclic carbonate groups was held constant for all the NIPU formulations, and the percentage of dopamine (DOP%) was calculated considering the total number of amino groups.

The sample containing 0.7 mol % DOP exhibited an improved adhesion (τ = 12.8 ± 1.3 MPa), with a 25% increment of the average lap-shear strength compared to the formulation without dopamine. On the other hand, the specimens with 1.3 and 1.9 mol % DOP presented a negligible increase in adhesion since the adhesion strength was 10.5 ± 1.0 and 10.7 ± 1.2 MPa, respectively. This lower adhesion was attributed to two counterproductive effects that emerged at higher dopamine hydrochloride contents: decrease in crosslink density due to the introduction of chain ends by monofunctional dopamine molecules and slower curing rate, resulting from the neutralization of DBU and therefore reduced availability of free catalyst to promote the reaction. The impact of dopamine hydrochloride on the

Published in : Macromolécules (2025)
DOI: 10.1021/acs.macromol.5c00718
Status : Postprint (Author's version)

cross-link degree was evidenced by gel content measurements after 1 day of RT curing (Table S4). While the effect was minimal in water, the gel content in THF clearly declined with increasing dopamine content, dropping from 74.3 ± 0.8% with 0.7 mol % DOP to 66.5 ± 0.8% with 1.9 mol % DOP. Thus, 0.7 mol % DOP represented an optimal concentration, at which dopamine's beneficial effects on interfacial adhesion were maximized without compromising the integrity of the polymer network or delaying its formation. All of the samples displayed a mixed adhesive-cohesive failure (Figure S43). These results clearly demonstrated that the incorporation of catechol groups into the matrix, even at low concentration, had a beneficial impact on the performance of the adhesive, and that dopamine could be used as an effective additional component in the solvent-free mixture.

The two commercial PU adhesives tested, TEROSON PU 6700 and ARALDITE 2028-1, provided solid bonding performance to aluminum, with average lap-shear strengths of 9.9 ± 1.1 and 8.2 ± 0.6 MPa, respectively. However, both products fell short in comparison to the NIPU formulations developed herein, especially those containing dopamine. This benchmarking study clearly showed that the solvent-free NIPU formulations presented in this work can exceed the adhesion strength of commercial PU adhesives, positioning them as a promising alternative for high-performance bonding applications.

Conclusions

The demand for isocyanate-free processes to prepare polyurethanes is particularly pressing in the field of adhesives and coatings, as the low reactivity of the starting reagents limits the curing of NIPU materials at ambient temperature. This work describes the development of novel NIPU solvent-free formulations that were completely cured at room temperature in a short time. Two-component mixtures were prepared using a liquid exovinylene bis(cyclic carbonate) and a low-viscosity polyamine cross-linker, and the rheological study of the polymerization showed that a suitable gel time at 25 °C was reached with 5 mol % catalyst loading. The reaction was monitored by infrared spectroscopy, which made evident that the cyclic carbonate was entirely converted after 3 days. Lowmolecular-weight liquid diamines were included in the composition to modulate the characteristics of the reticulated polymer system. To identify the type of linkages produced by the polyaddition and understand the effect of these diamines on the macromolecular properties, the corresponding linear polymers were synthesized. Linear NIPUs displayed dissimilar hydroxy-oxazolidone/oxo-urethane linkage selectivity and thermal properties, with a T_g ranging from −27 to 59 °C. Multiple mixtures were devised to produce cross-linked NIPUs, which were analyzed after 1 day and 7 days of RT curing. Fully cured thermosets were characterized by hydrophilic surfaces (contact angle between 60 and 74 °), great coating performance (samples classified as 5B or 4B), and a gel content that was high in water but moderate in THF (GC = 96.6 ± 0.3 and 79.5 ± 0.2%, respectively, for the most resistant thermosets). The $T_{deg10\%}$ was identified between 239 and 266 °C, and the T_g was always close to room temperature, between 10 and 24 °C. Tensile testing of freestanding NIPU films revealed that the polymer networks were stiffer and stronger when a larger quantity of diamine was used. Additionally, the thermosets

Published in : Macromolécules (2025)
DOI: 10.1021/acs.macromol.5c00718
Status : Postprint (Author's version)

became more ductile with time, often at the expense of their toughness. The bonding performance of NIPU adhesives was assessed by lap-shear testing on various substrates (aluminum, stainless steel, wood, PMMA, and HDPE), and the highest lap-shear strength was obtained with the most cross-linked material on aluminum alloy substrates (τ = 10.2 ± 0.2 MPa after 1 day of curing). The gluing properties for this formulation were also tested after integration of dopamine in the mixture, and a 25% increment of the lap-shear strength was achieved with 0.7 DOP% (τ = 12.8 ± 1.3 MPa). A benchmarking study against two commercial 2K solvent-free PU adhesives validated the results obtained with the NIPU formulations, which showed adhesion strength superior to that of traditional PU bonders. Although the synthesis of bisαCC incurs higher costs compared to conventional isocyanate-based products, its production process is scalable, and a similar approach could be applied to develop alternative liquid monomers. Further benefits could be achieved by replacing the cross-linker with other liquid biobased hardeners with tailored reactivity, which could potentially increase renewable content, enhance the degree of cross-linking, and eliminate the need for catalysts in the mixture. The fast hardening at room temperature constitutes a key advantage of the nonisocyanate polyurethanes developed in this work. Moreover, the long working time, ease of use, high adhesion performance, and solvent-free nature of the system highlight the sustainability and appeal of the process, which could be easily implemented as a cutting-edge 2K technology for room-temperature adhesives and coatings.

Associated Content

SUPPORTING INFORMATION

The Supporting Information is available free of charge at https://pubs.acs.org/doi/10.1021/acs.macromol.5c00718.

Rheology studies, 1H and 13C NMR spectra, IR spectra, SEC chromatograms, TGA and DSC curves, and tensile and lap-shear tests (PDF)

Published in : Macromolécules (2025)
DOI: 10.1021/acs.macromol.5c00718
Status : Postprint (Author's version)

Author Information

CORRESPONDING AUTHORS

Michael A. R. Meier - Institute of Organic Chemistry (IOC) and Institute of Biological and Chemical Systems-Functional Molecular Systems (IBCS-FMS), Karlsruhe Institute of Technology, Karlsruhe 76131, Germany ; orcid.org/0000-0002-4448-5279 ; Email: m.a.r.meier@kit.edu

Christophe Detrembleur - Center for Education and Research on Macromolecules (CERM), CESAM Research Unit, University of Liège, Liège 4000, Belgium; WEL Research Institute, Wavre 1300, Belgium ; orcid.org/0000-0001-7849-6796 ; Email: christophe.detrembleur@uliege.be

Author Contributions

L.N.: conceptualization, methodology, formal analysis, investigation, and writing. T.H.: conceptualization, methodology, and writing. Q.G.: resources. B.G. conceptualization, validation, supervision, and writing. M.A.R.M.: validation, supervision, and writing. C.D.: conceptualization, validation, supervision, and writing.

NOTES

The authors declare no competing financial interest.

Acknowledgments

This project has received funding from the European Union's Horizon 2020 Research and Innovation Program under the Marie Skłodowska−Curie Grant Agreement No. 955700. The authors from Liegè thank FNRS for the financial support in the frame of the CO2Switch project under Grant T.0075.20. C.D. is an F.R.S.-FNRS Research Director and thanks FNRS for financial support. The authors also thank Prof. Davide Ruffoni (University of Liege, Belgium) for giving access to the MTS equipment for realizing the lap-shear tests.

Published in : Macromolécules (2025)
DOI: 10.1021/acs.macromol.5c00718
Status : Postprint (Author's version)

References

1. Golling, F. E.; Pires, R.; Hecking, A.; Weikard, J.; Richter, F.; Danielmeier, K.; Dijkstra, D. Polyurethanes for Coatings and Adhesives – Chemistry and Applications. Polym. Int. 2019, 68 (5), 848– 855, DOI: 10.1002/pi.5665
2. The Business Research Company. Polyurethane Adhesives Global Market Report 2025 Https://Www.Thebusinessresearchcompany.Com/Report/Polyurethane-Adhesives-Global-Market-Report (accessed March 12, 2025).
3. Future Market Insights. Polyurethane Coating Market Growth – Trends & Forecast −2034 2024 Https://Www.Futuremarketinsights.Com/Reports/Global-Pu-Coatings-Market (accessed March 12, 2025).
4. European Commission. Commission Regulation (EU). 2020/1149 of 3 August 2020 Amending Annex XVII to Regulation (EC) No 1907/2006 of the European Parliament and of the Council Concerning the Registration, Evaluation, Authorisation and Restriction of Chemicals (REACH) as Regards Diisocyanates, 2020.
5. Rokicki, G.; Parzuchowski, P. G.; Mazurek, M. Non-Isocyanate Polyurethanes: Synthesis, Properties, and Applications: Non-Isocyanate Polyurethanes: Synthesis, Properties, and Applications. Polym. Adv. Technol. 2015, 26 (7), 707– 761, DOI: 10.1002/pat.3522
6. Kathalewar, M. S.; Joshi, P. B.; Sabnis, A. S.; Malshe, V. C. Non-Isocyanate Polyurethanes: From Chemistry to Applications. RSC Adv. 2013, 3 (13), 4110, DOI: 10.1039/c2ra21938g
7. Gomez-Lopez, A.; Panchireddy, S.; Grignard, B.; Calvo, I.; Jerome, C.; Detrembleur, C.; Sardon, H. Poly(Hydroxyurethane) Adhesives and Coatings: State-of-the-Art and Future Directions. ACS Sustainable Chem. Eng. 2021, 9 (29), 9541– 9562, DOI: 10.1021/acssuschemeng.1c02558
8. Panchireddy, S.; Thomassin, J.-M.; Grignard, B.; Damblon, C.; Tatton, A.; Jerome, C.; Detrembleur, C. Reinforced Poly(Hydroxyurethane) Thermosets as High Performance Adhesives for Aluminum Substrates. Polym. Chem. 2017, 8 (38), 5897– 5909, DOI: 10.1039/C7PY01209H
9. Cornille, A.; Michaud, G.; Simon, F.; Fouquay, S.; Auvergne, R.; Boutevin, B.; Caillol, S. Promising Mechanical and Adhesive Properties of Isocyanate-Free Poly(Hydroxyurethane). Eur. Polym. J. 2016, 84, 404– 420, DOI: 10.1016/j.eurpolymj.2016.09.048
10. Panchireddy, S.; Grignard, B.; Thomassin, J.-M.; Jerome, C.; Detrembleur, C. Catechol Containing Polyhydroxyurethanes as High-Performance Coatings and Adhesives. ACS Sustainable Chem. Eng. 2018, 6 (11), 14936– 14944, DOI: 10.1021/acssuschemeng.8b03429
11. Liu, C.; Wu, J.; Zhou, X.; Zhou, X.; Wu, Z.; Qu, J. Synthesis and Properties of Poly(Dimethylsiloxane)-Based Non-Isocyanate Polyurethanes Coatings with Good Anti-Smudge Properties. Prog. Org. Coat. 2022, 163, 106690 DOI: 10.1016/j.porgcoat.2021.106690
12. Wu, Z.; Tang, L.; Dai, J.; Qu, J. Synthesis and Properties of Fluorinated Non-Isocyanate Polyurethanes Coatings with Good Hydrophobic and Oleophobic Properties. J. Coat. Technol. Res. 2019, 16 (5), 1233– 1241, DOI: 10.1007/s11998-019-00195-5

13. Doley, S.; Dolui, S. K. Solvent and Catalyst-Free Synthesis of Sunflower Oil Based Polyurethane through Non-Isocyanate Route and Its Coatings Properties. Eur. Polym. J. 2018, 102, 161– 168, DOI: 10.1016/j.eurpolymj.2018.03.030

14. Panchireddy, S.; Grignard, B.; Thomassin, J.-M.; Jerome, C.; Detrembleur, C. Bio-Based Poly(Hydroxyurethane) Glues for Metal Substrates. Polym. Chem. 2018, 9 (19), 2650– 2659, DOI: 10.1039/C8PY00281A

15. Schmidt, S.; Ritter, B. S.; Kratzert, D.; Bruchmann, B.; Mülhaupt, R. Isocyanate-Free Route to Poly(Carbohydrate–Urethane) Thermosets and 100% Bio-Based Coatings Derived from Glycerol Feedstock. Macromolecules 2016, 49 (19), 7268– 7276, DOI: 10.1021/acs.macromol.6b01485

16. Monie, F.; Vidil, T.; Grau, E.; Grignard, B.; Detrembleur, C.; Cramail, H. The Multifaceted Role of Water as an Accelerator for the Preparation of Isocyanate-Free Polyurethane Thermosets. Macromolecules 2024, 57 (18), 8877– 8888, DOI: 10.1021/acs.macromol.4c01672

17. Bourguignon, M.; Thomassin, J.-M.; Grignard, B.; Jerome, C.; Detrembleur, C. Fast and Facile One-Pot One-Step Preparation of Nonisocyanate Polyurethane Hydrogels in Water at Room Temperature. ACS Sustainable Chem. Eng. 2019, 7, 12601– 12610, DOI: 10.1021/acssuschemeng.9b02624

18. Bourguignon, M.; Thomassin, J.; Grignard, B.; Vertruyen, B.; Detrembleur, C. Water-Borne Isocyanate-Free Polyurethane Hydrogels with Adaptable Functionality and Behavior. Macromol. Rapid Commun. 2021, 42 (3), 2000482 DOI: 10.1002/marc.202000482

19. Bourguignon, M.; Grignard, B.; Detrembleur, C. Introducing Polyhydroxyurethane Hydrogels and Coatings for Formaldehyde Capture. ACS Appl. Mater. Interfaces 2021, 13 (45), 54396– 54408, DOI: 10.1021/acsami.1c16917

20. Zhang, P.; Zhang, B.; Pan, J.; Zhang, G.; Ma, C.; Zhang, G. Ultrastrong and Versatile Nonisocyanate Polyurethane Adhesive under Extreme Conditions. Chem. Mater. 2023, 35, 7730, DOI: 10.1021/acs.chemmater.3c01517

21. Cornille, A.; Auvergne, R.; Figovsky, O.; Boutevin, B.; Caillol, S. A Perspective Approach to Sustainable Routes for Non-Isocyanate Polyurethanes. Eur. Polym. J. 2017, 87, 535– 552, DOI: 10.1016/j.eurpolymj.2016.11.027

22. Gomez-Lopez, A.; Elizalde, F.; Calvo, I.; Sardon, H. Trends in Non-Isocyanate Polyurethane (NIPU) Development. Chem. Commun. 2021, 57 (92), 12254– 12265, DOI: 10.1039/D1CC05009E

23. Capar, Ö.; Tabatabai, M.; Klee, J. E.; Worm, M.; Hartmann, L.; Ritter, H. Fast Curing of Polyhydroxyurethanes via Ring Opening Polyaddition of Low Viscosity Cyclic Carbonates and Amines. Polym. Chem. 2020, 11 (43), 6964– 6970, DOI: 10.1039/D0PY01172J

24. Besse, V.; Auvergne, R.; Carlotti, S.; Boutevin, G.; Otazaghine, B.; Caillol, S.; Pascault, J.-P.; Boutevin, B. Synthesis of Isosorbide Based Polyurethanes: An Isocyanate Free Method. React. Funct. Polym. 2013, 73 (3), 588– 594, DOI: 10.1016/j.reactfunctpolym.2013.01.002

25. Mokhtari, C.; Malek, C.; Manseri, A.; Caillol, S.; Negrell, C. Reactive Jojoba and Castor Oils-Based Cyclic Carbonates for Biobased Polyhydroxyurethanes. Eur. Polym. J. 2019, 113, 18– 28, DOI: 10.1016/j.eurpolymj.2019.01.039

26. Cornille, A.; Blain, M.; Auvergne, R.; Andrioletti, B.; Boutevin, B.; Caillol, S. A Study of Cyclic Carbonate Aminolysis at Room Temperature: Effect of Cyclic Carbonate Structures and Solvents on Polyhydroxyurethane Synthesis. Polym. Chem. 2017, 8 (3), 592– 604, DOI: 10.1039/C6PY01854H

27. Carré, C.; Bonnet, L.; Avérous, L. Original Biobased Nonisocyanate Polyurethanes: Solvent- and Catalyst-Free Synthesis, Thermal Properties and Rheological Behaviour. RSC Adv. 2014, 4 (96), 54018–54025, DOI: 10.1039/C4RA09794G

28. Lamarzelle, O.; Durand, P.-L.; Wirotius, A.-L.; Chollet, G.; Grau, E.; Cramail, H. Activated Lipidic Cyclic Carbonates for Non-Isocyanate Polyurethane Synthesis. Polym. Chem. 2016, 7 (7), 1439– 1451, DOI: 10.1039/C5PY01964H

29. Diakoumakos, C. D.; Kotzev, D. L. Non-Isocyanate-Based Polyurethanes Derived upon the Reaction of Amines with Cyclocarbonate Resins. Macromol. Symp. 2004, 216 (1), 37– 46, DOI: 10.1002/masy.200451205

30. Lambeth, R. H.; Henderson, T. J. Organocatalytic Synthesis of (Poly)Hydroxyurethanes from Cyclic Carbonates and Amines. Polymer 2013, 54 (21), 5568– 5573, DOI: 10.1016/j.polymer.2013.08.053

31. Tomita, H.; Sanda, F.; Endo, T. Polyaddition of Bis(Seven-membered Cyclic Carbonate) with Diamines: A Novel and Efficient Synthetic Method for Polyhydroxyurethanes. J. Polym. Sci., Part A: Polym. Chem. 2001, 39 (23), 4091– 4100, DOI: 10.1002/pola.10058

32. Blain, M.; Jean-Gérard, L.; Auvergne, R.; Benazet, D.; Caillol, S.; Andrioletti, B. Rational Investigations in the Ring Opening of Cyclic Carbonates by Amines. Green Chem. 2014, 16 (9), 4286– 4291, DOI: 10.1039/C4GC01032A

33. Dolci, E.; Michaud, G.; Simon, F.; Boutevin, B.; Fouquay, S.; Caillol, S. Remendable Thermosetting Polymers for Isocyanate-Free Adhesives: A Preliminary Study. Polym. Chem. 2015, 6 (45), 7851– 7861, DOI: 10.1039/C5PY01213A

34. Yuen, A.; Bossion, A.; Gómez-Bengoa, E.; Ruipérez, F.; Isik, M.; Hedrick, J. L.; Mecerreyes, D.; Yang, Y. Y.; Sardon, H. Room Temperature Synthesis of Non-Isocyanate Polyurethanes (NIPUs) Using Highly Reactive N-Substituted 8-Membered Cyclic Carbonates. Polym. Chem. 2016, 7 (11), 2105– 2111, DOI: 10.1039/C6PY00264A

35. Zhang, P.; Guo, H.; Qin, C.; Yuan, H.; Cao, Y.; Wang, Z.; Jin, C. Solvent-Free Synthesis of Bio-Based Non-Isocyanate Polyurethane (NIPU) with Robust Adhesive Property and Resistance to Low Temperature. Polym. Test. 2024, 140, 108616 DOI: 10.1016/j.polymertesting.2024.108616

36. Tounzoua, C. N.; Grignard, B.; Detrembleur, C. Exovinylene Cyclic Carbonates: Multifaceted CO2-Based Building Blocks for Modern Chemistry and Polymer Science. Angew. Chem., Int. Ed. 2022, 61 (22), e202116066 DOI: 10.1002/anie.202116066

37. Dabral, S.; Licht, U.; Rudolf, P.; Bollmann, G.; Hashmi, A. S. K.; Schaub, T. Synthesis and Polymerisation of α-Alkylidene Cyclic Carbonates from Carbon Dioxide, Epoxides and the Primary Propargylic Alcohol 1,4-Butynediol. Green Chem. 2020, 22 (5), 1553– 1558, DOI: 10.1039/C9GC04320A

38. Habets, T.; Siragusa, F.; Müller, A. J.; Grossman, Q.; Ruffoni, D.; Grignard, B.; Detrembleur, C. Facile Construction of Functional Poly(Monothiocarbonate) Copolymers under Mild Operating Conditions. Polym. Chem. 2022, 13 (21), 3076– 3090, DOI: 10.1039/D2PY00307D

39. Wong, A. R.; Barrera, M.; Pal, A.; Lamb, J. R. Improved Characterization of Polyoxazolidinones by Incorporating Solubilizing Side Chains. Macromolecules 2022, 55 (24), 11006– 11012, DOI: 10.1021/acs.macromol.2c02104

40. Gennen, S.; Grignard, B.; Tassaing, T.; Jérôme, C.; Detrembleur, C. CO2-Sourced α-Alkylidene Cyclic Carbonates: A Step Forward in the Quest for Functional Regioregular Poly (Urethane) s and Poly (Carbonate) s. Angew. Chem. 2017, 129 (35), 10530– 10534, DOI: 10.1002/ange.201704467

41. Habets, T.; Siragusa, F.; Grignard, B.; Detrembleur, C. Advancing the Synthesis of Isocyanate-Free Poly(Oxazolidones)s: Scope and Limitations. Macromolecules 2020, 53 (15), 6396– 6408, DOI: 10.1021/acs.macromol.0c01231

42. Habets, T.; Olmedo-Martínez, J. L.; Del Olmo, R.; Grignard, B.; Mecerreyes, D.; Detrembleur, C. Facile Access to CO 2 -Sourced Polythiocarbonate Dynamic Networks And Their Potential As Solid-State Electrolytes For Lithium Metal Batteries. ChemSusChem 2023, 16, e202300225 DOI: 10.1002/cssc.202300225

43. Razavi-Esfali, M.; Habets, T.; Siragusa, F.; Grignard, B.; Sardon, H.; Detrembleur, C. Design of Functional Isocyanate-Free Poly(Oxazolidone)s under Mild Conditions. Polym. Chem. 2024, 15 (19), 1962– 1974, DOI: 10.1039/D4PY00101J

44. Siragusa, F.; Crane, L.; Stiernet, P.; Habets, T.; Grignard, B.; Monbaliu, J.-C. M.; Detrembleur, C. Continuous Flow Synthesis of Functional Isocyanate-Free Poly(Oxazolidone)s by Step-Growth Polymerization. ACS Macro Lett. 2024, 13 (5), 644– 650, DOI: 10.1021/acsmacrolett.4c00203

45. Matos-Pérez, C. R.; White, J. D.; Wilker, J. J. Polymer Composition and Substrate Influences on the Adhesive Bonding of a Biomimetic, Cross-Linking Polymer. J. Am. Chem. Soc. 2012, 134 (22), 9498– 9505, DOI: 10.1021/ja303369p

46. Peykova, Y.; Lebedeva, O. V.; Diethert, A.; Müller-Buschbaum, P.; Willenbacher, N. Adhesive Properties of Acrylate Copolymers: Effect of the Nature of the Substrate and Copolymer Functionality. Int. J. Adhes. Adhes. 2012, 34, 107– 116, DOI: 10.1016/j.ijadhadh.2011.12.001

47. Brewis, D. M.; Mathieson, I.; Wolfensberger, M. Treatment of Low Energy Surfaces for Adhesive Bonding. Int. J. Adhes. Adhes. 1995, 15 (2), 87– 90, DOI: 10.1016/0143-7496(95)98742-5

48. Gomez-Lopez, A.; Grignard, B.; Calvo, I.; Detrembleur, C.; Sardon, H. Synergetic Effect of Dopamine and Alkoxysilanes in Sustainable Non-Isocyanate Polyurethane Adhesives. Macromol. Rapid Commun. 2021, 42 (3), 2000538 DOI: 10.1002/marc.202000538

49. Putnam, A. A.; Wilker, J. J. Changing Polymer Catechol Content to Generate Adhesives for High versus Low Energy Surfaces. Soft Matter 2021, 17 (7), 1999– 2009, DOI: 10.1039/D0SM01944E

50. Saiz-Poseu, J.; Mancebo-Aracil, J.; Nador, F.; Busqué, F.; Ruiz-Molina, D. The Chemistry behind Catechol-Based Adhesion. Angew. Chem., Int. Ed. 2019, 58 (3), 696– 714, DOI: 10.1002/anie.201801063

51. Sedó, J.; Saiz-Poseu, J.; Busqué, F.; Ruiz-Molina, D. Catechol-Based Biomimetic Functional Materials. Adv. Mater. 2013, 25 (5), 653– 701, DOI: 10.1002/adma.201202343